

7. Uneyama, K.; Morimoto, O.; Nanbu, H. *Tetrahedron Lett.* **1989**, 30, 109.
 8. Bouillon, J. P.; Maliverney, C.; Merenyi, R.; Viehe, H. G. *J. Chem. Soc., Perkin Trans. 1* **1991**, 2147.
 9. Nemeth, G.; Rakoczy, E.; Simig, G. *J. Fluorine Chem.*

1996, 76, 91.

10. Naac, D. G.; Burton, D. J. *J. Fluorine Chem.* **1971/1972**, 1, 123.

11. Suda, M. *Tetrahedron Lett.* **1981**, 22, 1421.

Orthocyclophanes. 7.¹ [1₄]Ketonand: Unexpected Formation and Its Rationalization by Calculation

Sungu Hwang, Gean Ha Ryua¹, Kwan Hee Lee, Jong-In Hong*, and Doo Soo Chung*

Department of Chemistry, Seoul National University, Seoul 151-742, Korea
 Received December 29, 1997

The chemistry of [1_n]orthocyclophane ([1_n]OCP) is of current interest in connection with the preparation of new macrocyclic compounds.¹⁻⁶ Systematic studies of [1_n]OCPs have shown that there are remarkable differences between the properties of even- and odd-numbered [1_n]OCPs—whereas oxidation of the benzylic methylenes in even-numbered [1_n]OCPdiones (n=6 or 8, **1** for n=6) provided the star-shaped cyclic polyketals ([1_n]starands, n=6 or 8, **2** for n=6)⁴ instead of the polyoxo [1_n]orthocyclophanes ([1_n]ketonands, **3** for n=6), oxidation of all remaining methylenes in odd-numbered [1_n]OCPdiones (n=5, 7, and 9) resulted in the formation of [1_n]ketonands (n=5, 7, and 9).⁵ This result suggested the generation of [1₄]starand from oxidation of [1₄]OCPdione (**4**). Herein, the unexpected formation of [1₄]ketonand (**5**) by oxidation of methylenes in [1₄]OCPdione (**4**) with ceric ammonium nitrate (CAN) is described and rationalized by semi-empirical quantum-mechanical MNDO calculations.

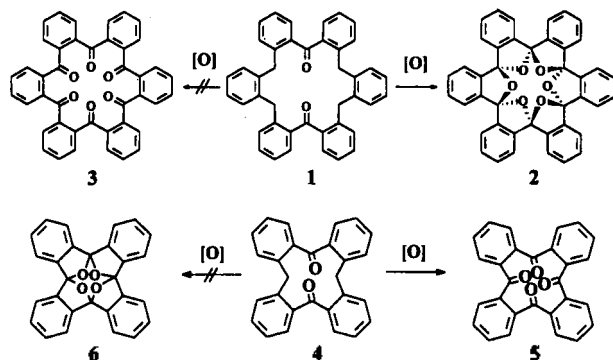
In contrast to oxidation of [1_n]OCPdiones (n=6 or 8), further oxidation of the dione **4** with CAN in hot CH₃CN for 6 days gave not the expected [1₄]starand (**6**), but [1₄]ketonand (**5**) in 61% yield.⁷ The formation of [1₄]ketonand was confirmed by spectroscopic evidence (vide infra).

The ¹³C NMR resonance at δ 194.06 and the IR ab-

sorption at 1660 cm⁻¹ revealed the presence of the carbonyl group. The exact mass (M⁺ 416.1049) agreed with the calculated value for C₂₆H₁₆O₄ (M 416.1046).

The energy calculation had been attempted by Cho *et al.* who had performed an *ab initio* study on model compounds in which the phenyl rings of **5** and **6** were replaced by simpler C=C bonds.⁸ In the present work, we carried out a semi-empirical quantum-mechanical MNDO calculation implemented in the GAMESS package^{9,10} on the full compounds without any simplification. The geometry was fully optimized in a C₁ symmetry (that is, without any symmetry restriction) by using the quasi-Newton-Raphson procedure¹¹ until a root-mean-square gradient less than 3.3 × 10⁻⁶ hartree/bohr (=0.0036 kcal/mol/Å) was reached. At each optimized geometry, all the vibrational frequencies were calculated to be real, indicating that the obtained structure corresponds to the true minimum. The optimized structure of **6** is in almost perfect agreement with that obtained by Cho *et al.*⁸ In the case of **5**, however, the direction of the carbonyl bonds was calculated to be somewhat different from those of Cho *et al.* This suggests the necessity of the explicit treatment of phenyl rings in the investigation of [1_n]OCPs, since the arrangement of oxygen atoms determines the cavity size, which is a very important property in their application as an ionophore.

The comparison of the energies of the two optimized structures shows that **5** is more stable than **6** by 76.8 kcal/mol. This is in good agreement with the *ab initio* results of Cho *et al.*,⁸ and supports the present experimental observation that **5** was formed instead of the expected **6**. The optimized structures are shown in Figures 1 and 2 in order to elucidate why **6** is less stable than **5**. The distances between the oxygen atoms were calculated to be around 2.3 Å for **6**, which are much shorter than the sum of van der Waals radii of two oxygen atoms, 3.0 Å (see the CPK representation in Figure 1b).¹² For **5**, the oxygen-oxygen distances were calculated to be 3.2-4.6 Å. Moreover, the calculation shows that each oxygen atom of **6** carries a slightly more negative charge of -0.34e than -0.27e of **5**. Thus, there is a larger electrostatic and steric repulsion between the oxygen atoms in **6** than **5**, and this explains in part why



¹Present address: The Institute of Natural Science, Sung Kyun Kwan University, Suwon, Kyungki-Do 440-746, Korea

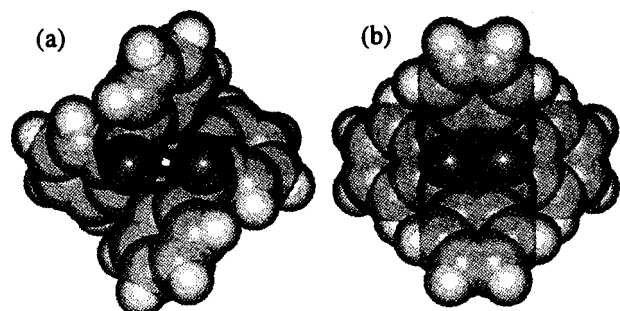
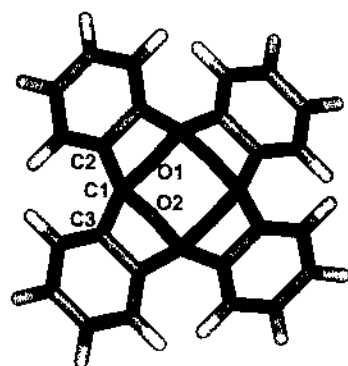


Figure 1. MNDO-optimized structures of (a) **5** and (b) **6**. The distance between the oxygen atoms is 3.2-4.6 Å for **5** and about 2.3 Å for **6**.

6 is less stable than **5**. Another source of the instability of **6** is the strain energy involved in the distortion needed to reduce the electrostatic and steric repulsion between the oxygen atoms. From Figure 2, we can see that the bond angles around the carbon atoms in the central cavity (C_4O_4) range from 96.4° to 138.7°, far from 109.5° of the ordinary sp^3 carbon.

In addition, the entropy change from **5** to **6** was estimated by performing free energy perturbation (FEP) calculations.¹³ The FEP method allows the calculation of the free energy difference (ΔA) between two similar structures having the same types of chemical bonds by slowly perturbing one structure into the other.¹⁴ For two systems having different types of bonds, however, only the contribution of the entropy ($-T\Delta S = \Delta A - \Delta E$) can be obtained from FEP calculations, since the force field used in the molecular mechanics (MM) and FEP calculations does not contain information about the absolute value of bond dissociation energy. The FEP calculation was carried out using the CVFF force field implemented in the Discover 95.0 molecular dynamics simulation package.¹⁵ 240 dynamic windows were used with the equilibration for 20 ps and the data collection for 20 ps at each window. The entire simulation was performed with a time step of 1.0 fs at 300 K in vacuum. The energy difference ΔE between the two isomers was calculated by MM calculations with the same CVFF force field as used in the FEP calculation. The free energy



	bond angle (in degree)
C2-C1-C3	138.7
C2-C1-O1	96.4
C2-C1-O2	107.2
O1-C1-O2	109.4

Figure 2. Bonding configurations around one of the carbon atoms forming the central cavity of **6**. The bond angles around the carbon atom range from 96.4° to 138.7°.

change ΔA from **5** to **6** was calculated to be 14.9 kcal/mol, and the energy difference was 15.2 kcal/mol. Thus the contribution of entropy ($-T\Delta S$) was estimated to be -0.3 kcal/mol. This has a negligible effect on the isomerism between **5** and **6**. However, the contribution of entropy to the isomerism is significant for larger $[1_n]$ ketonands and $[1_n]$ starands. Especially, the entropy change plays an important role to explain the formation of the $[1_7]$ ketonand instead of the $[1_7]$ starand, which will be reported later in detail.

Acknowledgment. This work was supported by the Basic Science Research Institute Program (BSRI-96-7403), the Organic Chemistry Research Center, and the Korea Science and Engineering Foundation (96-0501-08-01-3). We thank the late Prof. W. Y. Lee for advice, and Dr. Yun Hee Jang for her helpful discussion. S. H. gratefully acknowledges a postdoctoral research fellowship of Korea Research Foundation.

References

- Lee, K. H.; Hong, J.-I.; Lee, W. Y. Orthocyclophanes. 6. Hexamethoxy Derivatives of $[1_6]$ Orthocyclophane, *Bull. Korean Chem. Soc.* **1996**, 17(7), 661.
- (a) Lee, W. Y.; Sim, W.; Choi, K. D. *J. Chem. Soc., Perkin Trans. 1* **1992**, 881. (b) Lee, W. Y.; Sim, W.; Kim, H.-J. *J. Chem. Soc., Perkin Trans. 1* **1993**, 719. (c) Lee, W. Y.; Park, C. H.; Kim, E. H. *J. Org. Chem.* **1994**, 59, 4495. (d) Lim, C. W.; Hong, J.-I. *Bull. Korean Chem. Soc.* **1996**, 17(6), 558.
- Comprehensive presentations: (a) Izatt, R. M.; Christensen, J. J. *Synthetic Multidentate Macrocyclic Compounds*; Academic Press: New York, 1978. (b) Patai, S. *The Chemistry of Ethers, Crown Ethers, Hydroxy Groups and Their Sulfur Analogues*; John Wiley & Sons: Chichester, England, 1980; Parts 1 and 2. (c) Hiroaka, M. *Crown Compounds*; Kodansha Ltd.: Tokyo, and Elsevier Publishing Co.: Amsterdam, 1982. (d) Izatt, R. M. *Progress in Macrocyclic Chemistry*; John Wiley & Sons: New York, 1979, 1982; Vols. I and II. (e) Gokel, G. W.; Korzeniowski, S. H. *Macrocyclic Polyether Synthesis*; Springer-Verlag: Berlin, 1982. (f) Weber, E.; Toner, J. L.; Goldberg, I.; Vogtle, F.; Laidler, D. A.; Stoddart, J. F.; Bartsch, R. A.; Liotta, G. L. *Crown Ethers and Analogs*; John Wiley & Sons: Chichester, England, 1989. (g) Inoue, Y.; Gokel, G. W. *Cation Binding by Macrocycles*; Marcel Dekker, Inc.: New York, 1990. (h) Izatt, R. M.; Pawlak, K.; Bradshaw, J. S. *Chem. Rev.* **1991**, 91, 1721. (i) Weber, E., Ed. *Topics in Current Chemistry*; Springer-Verlag: Berlin, Heidelberg, 1991; Vol. 161.
- (a) Lee, W. Y.; Park, C. H.; Kim, S. *J. Am. Chem. Soc.* **1993**, 115, 1184. (b) Lee, W. Y.; Park, C. H. *J. Org. Chem.* **1993**, 58, 7149. (c) Lee, W. Y. *Synlett* **1994**, 765.
- Lee, W. Y.; Park, C. H.; Kim, H.-J.; Kim, S. *J. Org. Chem.* **1994**, 59, 878.
- Lee, W. Y.; Park, C. H.; Kim, Y. D. *J. Org. Chem.* **1992**, 57, 4074 and references therein.
- 2,9,16,23-Tetraoxopentacyclo[22.4.0.0^{3,8}.0^{10,15}.0^{17,22}]octacosane-1(24),3(8),4,6,10(15),11,13,17(22),18,20,25,27-dodecaene; $[1_4]$ Ketonand (**5**) A mixture of $[1_4]$ OCP-1,3-

dione **4** (40 mg, 0.1 mmol) and ceric ammonium nitrate (5.6 g) was heated at reflux temperature in CH_3CN for 6 days. After water was added to the reaction mixture, CH_3CN was removed *in vacuo*, and the residue was extracted with ether. The organic extract was washed with water, dried over MgSO_4 , concentrated *in vacuo*, and purified on SiO_2 (CH_2Cl_2) to give 25 mg of **5** (61% yield) as a crystalline solid: mp > 300 °C dec.; IR (KBr) 1660, 1640, 1580, 1280, 920 cm^{-1} ; ^1H NMR (CDCl_3 , 200 MHz) δ 7.35-7.51 (m, 16H, ArH); ^{13}C NMR (CDCl_3 , 50.29 MHz) δ 129.22, 131.71, 138.39, 194.06; EIMS m/z (relative intensity) 416 (88, M^+), 388 (8), 296 (100), 268 (30); HRMS (EI) calcd for $\text{C}_{28}\text{H}_{16}\text{O}_4$ 416.1046, found 416.1049.

8. Cho, S. J.; Hwang, H. S.; Park, J. M.; Oh, K. S.; Kim,

K. S. *J. Am. Chem. Soc.* **1996**, *118*, 485

9. Dewar, M. J. S.; Thiel, W. *J. Am. Chem. Soc.* **1977**, *99*, 4899.

10. Dupuis, M.; Spangler, D.; Wendoloski, J. J. NRCC Software Catalog, Vol. 1, Program No. QG01 (GAMESS) (University of California, Berkeley, CA, 1980).

11. Baker, J. J. *Comput. Chem.* **1986**, *7*, 385.

12. Bondi, A. J. *Phys. Chem.* **1964**, *68*, 441.

13. van Gunsteren, W. F. *Protein Eng.* **1988**, *2*, 5.

14. (a) Wunz, T. P. *J. Comput. Chem.* **1992**, *13*, 667. (b) Orozco, M.; Luque, F. J. *J. Am. Chem. Soc.* **1995**, *117*, 1378.

15. Discover User Guide, version 95.0. San Diego: Biosym Technologies, 1995.

Transformation of Nanoparticle Magnetite Prepared in Homogeneous Aqueous Solution

Hojun Kang, Choong Sub Lee[†], Don Kim, Young Soo Kang, and Yeong Il Kim*

Department of Chemistry, Pukyong National University, Pusan 608-737, Korea

[†]*Department of Physics, Pukyong National University, Pusan 608-737, Korea*

Received January 14, 1998

Recently nanoparticles of inorganic materials such as metal and semiconductor have been paid great attention due to the novel properties compared to their bulk materials.¹ Especially magnetic nanoparticles are of great interest for wide practical applications in information storage systems, catalysts, ferrofluids and medical diagnostics.² Among the several ultrafine magnetic particles many studies are devoted to nanoparticles of magnetite (Fe_3O_4) and maghemite ($\gamma\text{-Fe}_2\text{O}_3$). These iron oxides which have a size less than 10 nm were usually synthesized in various matrix materials such as polymers,³ micelles,⁴ vesicles⁵ and bilayer lipid membrane.⁶ They were also produced in homogeneous aqueous solution with very narrow size-distribution although the synthesis in an aqueous solution had been known to give larger particles.⁷ In those studies the synthesized nanoparticle magnetites, however, are not characterized well whether they are magnetite or maghemite or the mixture of two. Magnetite can be oxidized to maghemite and the oxidation proceeds by a topotactic reaction where the crystal structure is maintained throughout. Therefore the distinction between magnetite and maghemite is hardly possible from diffraction data in the case of small particle where the peak broadening is serious. At elevated temperature the transformation of magnetite to haematite ($\alpha\text{-Fe}_2\text{O}_3$) directly or *via* maghemite in air was studied in some details.⁸ At room temperature micrometer-sized magnetite is usually known to be stable in air and its oxidation to maghemite proceeds at surface over years.⁹ In the case of the particle whose size is less than 10 nm the surface components occupy significant parts of whole par-

ticle and diffusion pathway of oxygen is very short. The oxidation could be therefore significant. However, the oxidation of nanoparticle magnetite by air at room temperature has not been studied systematically yet.

In this communication we report the synthesis and transformation of nanoparticle Fe_3O_4 which is prepared in an aqueous homogeneous solution. Nanosized Fe_3O_4 has been prepared by dropping a solution mixture of FeCl_3 and FeCl_2 (molar ratio of $\text{Fe(III)/Fe(II)}=1.97$) in 0.4 M HCl slowly into 1.5 M NaOH solution while the resulting solution is vigorously stirred and the solution pH is kept to 11-12 by adding additional NaOH solution. After the iron mixture solution is all dropped the resulting suspension is kept stirred for 30 minutes. The precipitates are isolated using a magnet and transferred to deionized water. The suspension is centrifuged in 4000 rpm and washed again with deionized water. This procedure is repeated three times and finally washed with acetone. The resulting precipitates are dried in a vacuum for 5 hours at room temperature. All solutions are thoroughly deoxygenated by purging high purity N_2 for at least 30 minutes and the synthesis and all handling are done in N_2 -filled globe box.

Figure 1 shows the transmission electron microscopy (TEM) picture of the synthesized magnetite particles. The particles look spherical and have pretty even sizes. The average particle size is estimated to about 7.0 ± 1.2 nm from measuring 100 particles in the picture. This size is slightly smaller than that of magnetite nanoparticle previously prepared with a similar method by one of authors.⁷ Figure 2 (a)